Nucleic Acids Research, 1993, Vol. 21, No. 11 2683–2689

# Thermodynamics of DNA hairpins: contribution of loop size to hairpin stability and ethidium binding

Dionisios Rentzeperis, Karen Alessi and Luis A.Marky*
Department of Chemistry, New York University, New York, NY 10003, USA

Received January 13, 1993; Revised and Accepted March 25, 1993

## ABSTRACT

**A combination of calorimetric and spectroscopic techniques was used to evaluate the thermodynamic behavior of a set of DNA hairpins with the sequence d(GCGCT$_n$GCGC), where n = 3, 5 and 7, and the interaction of each hairpin with ethidium. All three hairpins melt in two-state monomolecular transitions, with $t_m$'s ranging from 79.1°C ($T_3$) to 57.5°C ($T_7$), and transition enthalpies of ~38.5 kcal mol$^{-1}$. Standard thermodynamic profiles at 20°C reveal that the lower stability of the $T_5$ and $T_7$ hairpins corresponds to a $\Delta G°$ term of +0.5 kcal mol$^{-1}$ per thymine residue, due to the entropic ordering of the thymine loops and uptake of counterions. Deconvolution of the ethidium-hairpin calorimetric titration curves indicate two sets of binding sites that correspond to one ligand in the stem with binding affinity, $K_b$, of ~$1.8 \times 10^6$ M$^{-1}$, and two ligands in the loops with $K_b$ of ~$4.3 \times 10^4$ M$^{-1}$. However, the binding enthalpy, $\Delta H_b$, ranges from −8.6 ($T_3$) to −11.6 kcal mol$^{-1}$ (T7) for the stem site, and −6.6 ($T_3$) to −12.7 kcal mol$^{-1}$ ($T_7$) for the loop site. Relative to the $T_3$ hairpin, we obtained an overall thermodynamic contribution (per dT residue) of $\Delta\Delta H_b = \Delta(T\Delta S_b) = -0.7_5$ kcal mol$^{-1}$ for the stem sites and $\Delta\Delta H_b = \Delta(T\Delta S_b) = -1.5$ kcal mol$^{-1}$ for the loop sites. Therefore, the induced structural perturbations of ethidium binding results in a differential compensation of favorable stacking interactions with the unfavorable ordering of the ligands.**

## INTRODUCTION

Hairpin structures are a common feature of RNA molecules (1, 2), and their formation in DNA molecules has been postulated in regions with palindromic sequences, which have been implicated in gene regulation (3–5). The overall structure and physical properties of small single-stranded hairpin molecules as well as the effects of sequence and loop size on hairpin stability have been reported earlier (6–22). These hairpin molecules are useful for thermodynamic studies because they form stable duplexes that are partially paired over a convenient temperature range and tend to melt in monomolecular transitions.

Intercalative binding of drugs to nucleic acid duplexes has been studied extensively by a wide range of experimental techniques. Structural studies of drug–DNA complexes have shown that most intercalators bind to DNA duplexes with a sequence preference for a 5′-Pyr-Pur-3′ site and neighbor exclusion of at least two base pairs (23–25). For instance, the binding of ethidium in solution to hexamers containing G·C base pairs follows this rule, as demonstrated by Krugh and coworkers (26). Our research efforts focus on investigating the effect of loop size on both the thermodynamics of the helix-coil transition of short single-stranded DNA hairpins and ligand binding to these hairpins. We present here a complete thermodynamic description of the melting behavior of three hairpin molecules with sequence d(GCGCT$_n$GCGC), where n = 3, 5 and 7, designated as $T_3$, $T_5$ and $T_7$ hairpins, respectively, as well as the interaction of ethidium, Figure 1, with these molecules. Our thermodynamic results demonstrate that all three hairpin molecules melt in two-state transitions with similar enthalpies of ~38.5 kcal mol$^{-1}$. The decrease in thermal stability from 79.1°C to 57.5°C as the loop size is increased from 3 to 7 thymine residues corresponds to the unfavorable ordering of the thymine loops. Ethidium interacts with these hairpin molecules in two different binding modes: by intercalation of one ligand in the center of the stem, and by a weaker association of two ligands to the loop. The induced structural perturbations of ethidium binding results in a differential compensation of favorable stacking interactions with the unfavorable ordering of the ligands. Relative to the $T_3$ hairpin, this amounts to a thermodynamic contribution (per dT residue) of $\Delta\Delta H_b = \Delta(T\Delta S_b) = -0.7_5$ kcal mol$^{-1}$ for the stem sites, and $\Delta\Delta H_b = \Delta(T\Delta S_b) = -1.5$ kcal mol$^{-1}$ for the loop sites.

## MATERIALS AND METHODS

### Chemicals

All deoxyoligonucleotides were synthesized on an ABI 391 automated synthesizer, using standard phosphoramidite chemistry (27), purified by HPLC, and desalted on a Sephadex G-10 exclusion chromatography column. The following extinction coefficients of the oligomers at 260 nm and 95°C, in M$^{-1}$cm$^{-1}$,

* To whom correspondence should be addressed

were determined in water by a procedure described earlier (28, 29): $T_3$, $\epsilon = 0.91\times10^5$; $T_5$, $\epsilon = 1.08\times10^5$; and $T_7$, $\epsilon = 1.24\times10^5$. Ethidium bromide was obtained from Sigma and used without further purification. The concentration of this ligand was determined using the molar extinction coefficient of 5,850 $M^{-1}cm^{-1}$ at 480 nm (30). All other chemicals were reagent grade. The buffer solutions consisted of 10 mM sodium phosphate (NaPi), 0.1 mM $Na_2EDTA$ at pH 7.0 and adjusted to the desired ionic strength with NaCl.

### Temperature-dependent UV spectroscopy

Absorbance versus temperature profiles (melting curves) in appropriate solution conditions were measured at 275 nm with a thermoelectrically controlled Perkin-Elmer 552 spectrophotometer, interfaced to a PC-XT computer for the acquisition and analysis of experimental data. The temperature was scanned at a heating rate of 1.0°C $min^{-1}$. Melting curves were carried out as a function of strand concentration and salt concentration (at constant strand concentration). The analysis of these melting curves, using standard procedures described earlier (17, 31), allows us to measure transition temperatures, $T_m$, van't Hoff enthalpies, $\Delta H_{vH}$, and the release of counterions, $\Delta n_{Na^+}$.

### Differential scanning calorimetry

Excess heat capacity as a function of temperature (DSC melts) were measured with a Microcal MC-2 differential scanning calorimeter (Northampton, MA). Two cells, the sample cell containing 1.5 mL of oligomer solution and the reference cell filled with buffer solution, were heated from 5°C to 110°C at a heating rate of 0.75°C $min^{-1}$. Analysis of the resulting thermograms, using procedures described previously (31), allows us to obtain standard thermodynamic profiles ($\Delta H$, $\Delta S$, and $\Delta G°$) and model-dependent enthalpies, $\Delta H_{vH}$, of the helix−coil transition of all three DNA hairpins.

### Isothermal titration calorimetry

The heats of interaction of ethidium bromide with each hairpin molecule were measured directly by titration calorimetry using the Omega calorimeter from Microcal Inc. Ethidium solutions, with a 40-fold higher concentration than the hairpin solution in the reaction cell, were used to titrate each hairpin with a 100 μL syringe. Complete mixing was effected by stirring of the syringe paddle at 400 rpm. The reference cell of the calorimeter was filled with water and the instrument calibrated by means of a known standard electrical pulse. An average of 28 injections of 5 μL each were performed in a single titration. The area of the peak following each injection is proportional to the interacting heat, Q. This heat corrected for the dilution heat of the ligand and normalized by the concentration of added titrant, is equal to the binding enthalpy, $\Delta H_b$. The precision of the resulting heat of each injection is less than 0.5 μcal. A better and independent determination of $\Delta H_b$ is to average several intermediate peaks that correspond to a particular site. Analysis of the calorimetric binding isotherm allows us to obtain, in addition to the binding enthalpy, binding affinities and the overall stoichiometry of the complexes (described in a latter section).

### Stoichiometry of ethidium−hairpin complexes

The stoichiometry of the complexes of ethidium with each of the three hairpins was determined primarily by titration calorimetry experiments as described in the next section. Alternatively, these

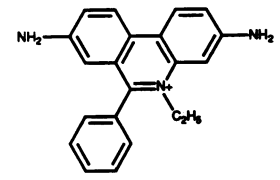


**Figure 1.** Structure of ethidium.

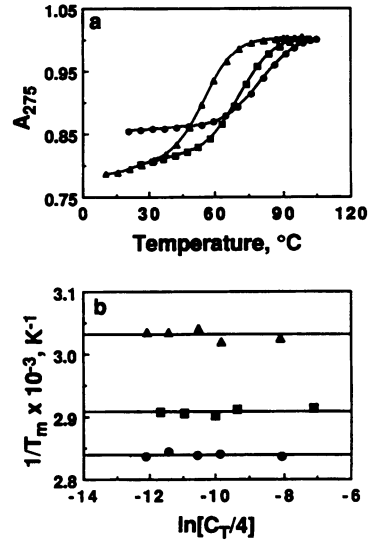


**Figure 2. a)** Normalized melting curves of the hairpins (50 μM in strand concentration) in 10 mM NaPi buffer, 0.1 mM $Na_2EDTA$, at pH 7. **b)** Dependence of $T_m$ on strand concentration. Hairpin $T_3$ (●), $T_5$ (■), and $T_7$ (▲).

stoichiometries were measured spectroscopically using the method of continuous variations in which a hairpin solution is titrated with ligand at constant total concentration of hairpin and ligand (26). The experimental observable is the change in absorbances at 480 nm and 540 nm, as a function of the mole fraction of hairpin. The intersections of the two lines of absorbance vs. mole fraction of hairpin plots represent mole fraction values that correspond to the stoichiometry of the complexes.

### Determination of ligand association constants

Ethidium binding constants were measured from analysis of the calorimetric binding isotherms and from the increase in thermal stability of the saturated ligand−DNA complexes relative to the free oligomer duplexes. The first method is based on the binding of a ligand to oligomers containing two types of independent binding sites: the intercalation site at the center of the stem and the additional sites of the thymine loops. Each type of site is characterized by an equilibrium constant, $K_b$, binding enthalpy, $\Delta H_b$, and apparent number of ligands per binding site, n. The experimental calorimetric binding isotherm is the dependence of the total heat, $Q_T$, on the total concentration of ligand added, $X_T$. The above three parameters for each type of site are determined iteratively using the Marquardt algorithms as described previously (32). The initial fitting procedure lets all three parameters float or fixes either the enthalpy, determined

**Table 1.** Spectroscopic and calorimetric melting results[a]

| Hairpin | UV | | Calorimetry | | | | | |
|---|---|---|---|---|---|---|---|---|
| | $t_m$ (°C) | $\Delta H_{vH}$ (kcal mol$^{-1}$) | $t_m$ (°C) | $\Delta H_{vH}$ (kcal mol$^{-1}$) | $\Delta H_{cal}$ (kcal mol$^{-1}$) | $\Delta G°$ (kcal mol$^{-1}$) | $T\Delta S$ (kcal mol$^{-1}$) | $\Delta n_{Na^+}$ mol $Na^+$ / mol Pi |
| $T_3$ | 79.5 | −39 | 79.1 | −38 | −38.1 | −6.4 | −31.7 | 0.04 |
| $T_5$ | 71.0 | −38 | 69.2 | −38 | −39.2 | −5.6 | −33.6 | 0.05 |
| $T_7$ | 56.7 | −41 | 57.5 | −39 | −38.2 | −4.3 | −33.9 | 0.05 |

[a]All thermodynamic parameters refer to the formation of hairpins in 10 mM sodium phosphate buffer, 0.1 mM $Na_2EDTA$ at pH 7.0 and 20°C. The $t_m$'s (±0.5°C) corresponds to strand concentrations of 5−50 μM for the UV melts, and 300 μM ($T_3$ and $T_7$) and 800 μM ($T_5$), for the DSC melts. The values given in parenthesis are the absolute uncertainties of: $\Delta H_{vH}$ (±7%); $\Delta H_{cal}$ (±3%); $\Delta G°$(±5%); $T\Delta S$ (±8%); and $\Delta n_{Na^+}$ (±5.0%).

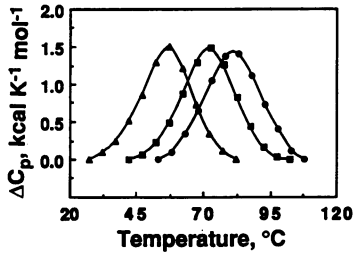


**Figure 3.** Typical excess molar heat capacity curves relative to buffer consisting of 10 mM NaPi buffer, 0.1 mM $Na_2EDTA$, at pH 7. Hairpin $T_3$ (●), $T_5$ (■), and $T_7$ (▲). At strand concentrations of 300 μM for $T_3$ and $T_7$ and 800 μM for $T_5$.

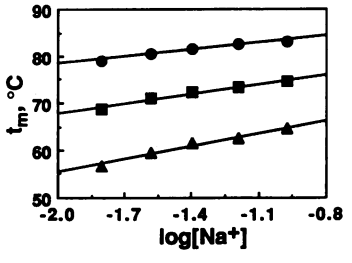


**Figure 4.** Salt dependence of the $t_m$ for all three hairpin molecules in 10 mM NaPi buffer, 0.1 mM $Na_2EDTA$ at pH 7 adjusted to the desired NaCl concentration. Hairpin $T_3$ (●), $T_5$ (■), and $T_7$ (▲).

independently by averaging the heats of the intermediate peaks of a given site, or n parameters or both until the lowest standard deviation of the fit is obtained; all approaches result in similar values.

The thermal stabilization of the 1:1 ethidium−hairpin complex, $35\Delta T_m$, relative to free hairpin follows the equation (33): $\Delta T_m = (T°_m\ T_m/n'\ R\ \Delta H_{bs})\ \ln(1+Ka_L)$ where $T°_m$ and $T_m$ are the transition temperatures of the free and 1:1 complexes, respectively; $\Delta H_{bs}$, the formation enthalpy of the base-pair stacks covered by the ligand; $a_L$, the activity of the free ligand at $T = T_m$, is assumed equal to one half of the total concentration of ethidium; n', the apparent number of ligand per binding site. Ligand binding affinities are extrapolated to 20°C by the equation: $d\ln K_b/dT = \Delta H_b(T)/RT^2$, where $\Delta H_b$ (T) is the binding enthalpy at temperature T, equal to: $\Delta H_{b,293} + \int \Delta C_p dT$. In the last equation we used a $\Delta C_p$ value of −87 $calK^{-1}\ mol^{-1}$. This value was determined experimentally by calorimetric titrations of the $T_5$ hairpin with ethidium in the temperature range of 5°C to 30°C (34).

## RESULTS

### THERMODYNAMIC CHARACTERISATION OF SINGLE-STRANDED HAIRPINS

#### Helix−coil transitions of hairpins

The helix−coil transition of the ordered structures formed by each hairpin was characterized initially by UV melting curves. The transition temperatures and the corresponding van't Hoff enthalpies for all three hairpins are listed in Table 1. The melting of all three molecules occurs in broad monophasic transitions with hyperchromicities, at 275 nm, of 15%, 20% and 22% for the $T_3$, $T_5$ and $T_7$ hairpins, respectively, see Figure 2a; and van't Hoff transition enthalpies of ~39 kcal $mol^{-1}$. In these optical melts, a ten-fold increase in oligomer concentration has no effect on the $t_m$ of the oligomers, see Figure 2b, consistent with the unimolecular melting of single-stranded hairpins. Typical excess heat capacity versus temperature profiles are shown in Figure 3. The $t_m$'s, $\Delta H_{cal}$ and $\Delta H_{vH}$ values obtained from these curves are listed in Table 1. Figure 3 shows results of DSC thermograms that are all monophasic with no changes in heat capacities within the initial and final states. In spite of the 60-fold ($T_3$, and $T_7$ hairpins) or 160-fold ($T_5$ hairpin) increase in strand concentration relative to the concentration used in optical melts, the $t_m$ remains the same. Assuming a negligible enthalpic contribution of the loop, the average $\Delta H_{cal}$ of 38.5 kcal $mol^{-1}$ for all hairpins is in good agreement with the enthalpies of 34.1 kcal $mol^{-1}$ estimated from DNA nearest-neighbor parameters determined in 1 M NaCl (35). Comparison of the model-dependent $\Delta H_{vH}$'s calculated from calorimetric or optical experiments and $\Delta H_{cal}$ for a given molecule allows us to draw conclusions about the nature of the transitions (31). We obtained $\Delta H_{vH}/\Delta H_{cal}$ ratios of 0.97−1.02 for all hairpins; the $\Delta H_{vH}$ values corresponds to the melting of one cooperative unit size. Therefore, all hairpins melt in two-state transitions.

#### Salt dependence of $T_m$ and overall counterion release

Figure 4 shows the dependence of the transition temperature on salt concentration, $t_m$ vs. log [$Na^+$] plots. We obtained values ranging from 4.9−9.0°C for the slopes of such plots. This weak dependence on salt concentration is characteristic of ion releases occurring in short oligomeric duplexes (17, 36). Since we measure the transition enthalpies for each hairpin by DSC, we can calculate $\Delta n_{Na^+}$ per phosphate using procedures described

**Table 2.** Fitting analysis of calorimetric binding isotherms[a]

| Hairpin | Stem n mol ligand / mol DNA | $\Delta H_b$ (kcal mol$^{-1}$) | $K_b$ ($M^{-1}$) | Loop n mol ligand / mol DNA | $\Delta H_b$ (kcal mol$^{-1}$) | $K_b$ ($M^{-1}$) | $\sigma$ (%) |
|---|---|---|---|---|---|---|---|
| $T_3$ | 1.0 | −8.6 | $1.2\times10^6$ | 2.0 | −6.6 | $2.9\times10^4$ | 1.3 |
| $T_5$ | 0.9 | −9.8 | $1.7\times10^6$ | 1.8 | −8.9 | $6.5\times10^4$ | 10.2 |
| $T_7$ | 1.0 | −11.6 | $2.5\times10^6$ | 2.0 | −12.7 | $3.5\times10^4$ | 6.0 |

[a]All values in 10 mM sodium phosphate buffer, 0.1 mM $Na_2EDTA$, at pH = 7.0 and 20°C. $\sigma$ is the standard deviation of the non-linear fits.

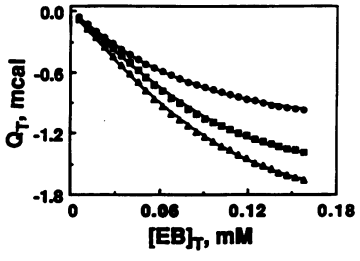


**Figure 5.** Calorimetric binding isotherms curves in 10 mM NaPi buffer, 0.1 mM $Na_2EDTA$, at pH 7. Hairpin $T_3$ (●), $T_5$ (■), and $T_7$ (▲); 1.4 mL of oligomer solution at strand concentration of 40 μM titrated with 5 μL aliquots of a 1.6 mM solution of ethidium bromide.

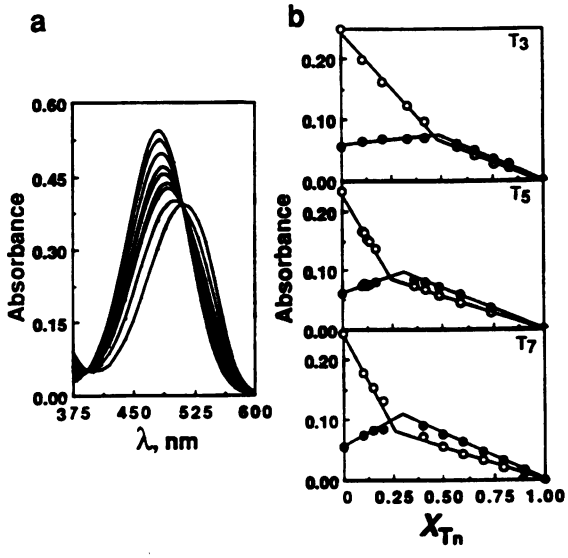


**Figure 6.** a) Typical visible spectra of the ethidium-$T_5$ complexes in 10 mM NaPi buffer, 0.1 mM $Na_2EDTA$ at pH 7 and 20°C. b) Each panel corresponds to the resulting Job plots of ethidium with the indicated hairpin. Absorbances were monitored at two wavelengths, 480 nm (m) and 540 nm (●), using a cell with a 1 cm pathlength. The concentration of ethidium plus hairpin was kept constant at 40 μM throughout the experiments.

previously (17, 37), by taking into account the phosphates of both the helical stem and loop of each hairpin molecule. We obtained $\Delta n_{Na^+}$ values ranging from 0.04 to 0.05 mole of $Na^+$ per mole of phosphate (see Table 1) when we take into account all the phosphates of each molecule. Alternatively, if only the 6 helical phosphates of the stem are taken into account, the resulting $\Delta n_{Na^+}$ values range from 0.06 to 0.13 mole of $Na^+$ per mole of phosphate. Thus, although the helical stem is identical in the hairpins, additional thymines in the loop increases the overall counterion uptake and corresponds to an increase of stacking interactions between thymine residues and/or the formation of additional base-pair stacks of thymine residues on the helical stems, as has been reported previously in the binding of netropsin to the loops of DNA dumbbell molecules (38).

## Standard thermodynamic profiles of hairpin formation at 20°C

For suitable comparisons Table 1 lists standard thermodynamic profiles for the formation of each molecule at 20°C, a temperature at which all molecules are fully ordered. The $\Delta S$ and $\Delta G°$ are calculated directly from DSC experiments with the equations: $\Delta S = \int (\Delta Cp/T)\, dT$ and $\Delta G° = \Delta H_{cal} - 293.15\ \Delta S$; in the Gibbs equation, both the enthalpy and entropy are assumed to be independent of temperature, i.e. $\Delta C_p = 0$. For all hairpins, the $\Delta G°$ values determined in this way follow the equation: $\Delta G° = \Delta H_{cal}\ (1-293.15/T_m)$ closely, which is rigorously true for the monomolecular folding of single-stranded hairpins. Inspection of Table 1 indicates that the favorable free energy term for each molecule is the result of a partial enthalpy−entropy compensation. The increase in the number of thymine residues in the loop results in a less favorable $\Delta G°$ term of $+0.5_3$ kcal per residue, in agreement with previous results (39). This destabilization is entropy driven and corresponds to both the ordering of the thymine residues and an increase in counterion uptake by the loop.

## ETHIDIUM BINDING TO THE STEM AND LOOP SITES OF HAIRPINS

### Titration calorimetry

The integral heat as a function of total added ligand for all ethidium−hairpin systems and the resulting fitted curves are shown in Figure 5. Molar binding enthalpies for the high affinity sites ($\sim 10^6$) in the stem of these molecules were calculated by averaging the heats of the first few points of these isotherms (or from the fits of these calorimetric titrations) which correspond to complete binding of ligand. These values are listed under the $\Delta H_b$ columns in Table 2. Inspection of this column shows that binding of ethidium to all three molecules is accompanied by an exothermic enthalpy ranging from −8.6 kcal mol$^{-1}$ to −11.6 kcal mol$^{-1}$. The analysis of the calorimetric binding isotherms shows binding affinities in good agreement with the ones obtained from optical melts of the 1:1 ethidium−hairpin complexes. In addition, in these calorimetric titrations we were able to detect secondary, weaker sites for ethidium in the hairpins, see Table 2. These sites may be located at the loops of each hairpin,

**Table 3.** Spectroscopic binding affinities of ethidium–hairpin complexes[a]

| Hairpin | $T^{\circ}_m$ (K) | $T_m$ (K) | n' | $\Delta H_{bs}$ (kcal mol$^{-1}$) | $\Delta H_b$ (kcal mol$^{-1}$) | $K_b$ ($M^{-1}$) |
|---|---|---|---|---|---|---|
| $T_3$ | 352.25 | 355.70 | 1 | −11.9 | −8.6 | $2.1\times10^6$ |
| | (356.23) | (357.96) | 1 | −11.9 | −8.6 | $(1.1\times10^6)$ |
| $T_5$ | 340.82 | 348.29 | 1 | −11.9 | −9.8 | $2.3\times10^6$ |
| | (347.71) | (350.08) | 1 | −11.9 | −9.8 | $(8.0\times10^5)$ |
| $T_7$ | 329.90 | 337.11 | 1 | −11.9 | −11.6 | $1.9\times10^6$ |
| | (337.65) | (338.75) | 1 | −11.9 | −11.6 | $(2.7\times10^5)$ |

[a]$K_b$'s were estimated from the observed increase in the thermal stability of the ethidium–DNA complexes relative to the free DNAs. $\Delta H_b$ was obtained from titration calorimetry and $\Delta H_{bs}$ is the enthalpy of formation of the CG/CG base-pair stack from nearest neighbors parameters (35). All experiments were done in 10 mM sodium phosphate buffer, 0.1 mM $Na_2EDTA$, at pH = 7.0 and 20°C (values in parenthesis with addition of 0.1 M NaCl). $T_m$'s are within ±0.5K, n' is within (±10%), and $K_b$ ~ ±50% of the absolute values.

composed of the constrained thymines of these loops. The interesting observation is that each loop is able to accommodate up to two additional ligand molecules. These sites are characterized with $K_b$'s of ~$10^4$ and average $\Delta H_b$'s ranging from −6.6 kcal mol$^{-1}$ to −12.7 kcal mol$^{-1}$.

## UV spectra and overall stoichiometry of ethidium–hairpin complexes

Figure 6a shows the typical UV spectra of a ethidium and ethidium-$T_5$ complexes in solution. The addition of hairpin to an ethidium solution results in changes in the overall UV spectrum. In particular we obtained the characteristic red shift of the bound ligand, ~40 nm, and the presence of two isosbestic points at 390 nm and 510 nm, as has been reported previously (40). At the wavelengths of maximum changes in the absorbance of the free and bound ligands, 480 nm and 540 nm, we have followed the changes in absorbance as a function of the mole fraction of hairpin, $X_{Tn}$. The resulting Job plots are shown in Figure 6b. The intersection of the two lines in each titration curve at the more sensitive wavelength of 480 nm occurs at $X_{Tn}$ values of 0.51, 0.25 and 0.26 (0.49, 0.30 and 0.30 at 540 nm) for the $T_3$, $T_5$ and $T_7$ hairpins, respectively; and corresponds roughly to stoichiometries of 1:1 (ethidium molecules per hairpin) for the ethidium complex with $T_3$ and 3:1 for the complex of ethidium with $T_5$ and $T_7$. At 277 nm (where both DNA and ethidium absorb light) we obtained stoichiometries of 2:1 with $T_3$ and 3:1 for the other two hairpins (data not shown). Overall, these values are in excellent agreement with the stoichiometries obtained from titration calorimetry, except for the lower stoichiometry with the $T_3$ hairpin. This may be because the thymines in the $T_3$ hairpin are completely exposed to solvent, as was determined by NMR analysis with a similar loop sequence (41). Ethidium partially stacks to these thymine bases resulting therefore in reduced spectral changes. This observation is consistent with the lower hyperchromicity of $T_3$ and the reduced binding enthalpy in its interaction with ethidium.

## Ethidium binding affinities

Although all ethidium binding affinities were extracted from the fits of the calorimetric isotherms, we have used a second method, the increase in thermal stability of the 1:1 ethidium–hairpin relative to the free hairpins, to estimate the $K_b$'s for the high affinity site of the stem. Table 3 lists the specific parameters used and the resulting $K_b$'s obtained at two different salt concentrations. In low salt we obtained similar $K_b$ values of

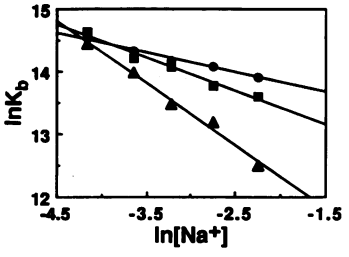


**Figure 7.** Salt dependence of ethidium binding affinities with hairpins in 10 mM NaPi buffer, 0.1 mM $Na_2EDTA$ at pH 7 and 20°C, and adjusted to the desired NaCl concentration. Hairpin $T_3$ (●), $T_5$ (■), and $T_7$ (▲).

~$10^6$ for all three hairpins; these values are in excellent agreement with the ones obtained from titration calorimetry. The magnitude (42) and the similarity of these binding affinities for all three molecules strongly indicates that this site remains unperturbed and is consistent with the intercalative binding of ethidium to the central CG/CG base-pair stack in the stem of these hairpins. With a tenfold increase in NaCl concentration, the $K_b$'s decreased to ~$10^5$, the actual values of the slopes of the ln $K_b$ vs. ln [$Na^+$] lines of Figure 7 range from −0.32 to −0.99; the theoretical value for this ligand calculated from polyelectrolyte theory ranges from −1.00 to −1.24 (37, 43). Therefore, our experimental values for the release of counterions per one bound ethidium are in qualitative agreement with the lower charge density of the unligated hairpins. For the second type of binding sites in the loop, we were unable to measure the corresponding $K_b$'s from melting curves because of the small further increment in the $t_m$ of the 2:1 and 3:1 ethidium–hairpin complexes, ~1–2°C, and the much lower magnitude of these binding affinities, ~$10^4$.

## Thermodynamic profiles for ethidium binding

Values for the thermodynamic profiles for the binding sites of ethidium to each of the three hairpin duplexes at 20°C are listed in Table 4. In this table we have tabulated standard thermodynamic profiles, $\Delta G^{\circ}_b$, $\Delta H_b$, $T\Delta S_b$ for the stem and loop sites and dln $K_b$/dln [$Na^+$] for the site at the stem. The $\Delta G^{\circ}_b$ was derived from the values of $K_b$ according to $\Delta G^{\circ}_b = -RT \ln K_b$. The entropy changes, $T\Delta S_b$, were then calculated from the Gibbs equation. For these binding sites, we obtained

Table 4. Thermodynamic profiles for ethidium binding to hairpins[a]

| Hairpin | Site | $\Delta G°_b$ (kcal mol$^{-1}$) | $\Delta H_b$ (kcal mol$^{-1}$) | $T\Delta S_b$ (kcal mol$^{-1}$) | $d\ln K_b/d\ln [Na^+]$ (mol $Na^+$/mol EB) |
|---|---|---|---|---|---|
| $T_3$ | stem | −8.2 | −8.6 | −0.4 | −0.315 |
| | loop | −6.0 | −6.6 | −0.6 | – |
| $T_5$ | stem | −8.4 | −9.8 | −1.4 | −0.533 |
| | loop | −6.5 | −8.9 | −2.4 | – |
| $T_7$ | stem | −8.6 | −11.6 | −3.0 | −0.993 |
| | loop | −6.1 | −12.7 | −6.6 | – |

[a]Values taken in 10 mM sodium phosphate buffer, 0.1 mM $Na_2EDTA$ at pH = 7.0 and 20°C. The $\Delta G°_b$ values are within (±5%), $\Delta H_b$ (±3%), and $T\Delta S_b$ (±8%).

average $\Delta G°_b$ of −8.4 kcal mol$^{-1}$ and −6.2 kcal mol$^{-1}$ for the stem and loop sites, respectively, that correspond to binding processes that are primarily enthalpic driven. However, relative to the $T_3$ hairpin, the small decrease in the favorable $\Delta G°_b$ terms with the increase in number of thymines of the other two hairpin molecules corresponds to a nearly enthalpy−entropy compensation for the two types of binding sites, equal to $\Delta\Delta H_b = \Delta(T\Delta S_b) = -0.7_5$ kcal mol$^{-1}$ for the stem sites, and $\Delta\Delta H_b = \Delta(T\Delta S_b) = -1.5$ kcal mol$^{-1}$ for the loop sites. The values of these differential compensating terms for the loop sites are twice the values of the stem sites; this effect is consistent with the higher ordering of ethidium molecules in the loops of these molecules.

## DISCUSSION

### Exclusive formation of intramolecular hairpins

The sequence of d(GCGCT$_n$GCGC) favors the exclusive formation of intramolecular duplexes. The formation of intermolecular duplexes would involve four G·C base pairs interspaced by internal loops of 6, 10 and 14 thymine residues each, which would render them unstable. The $t_m$'s for the helix−coil transition of each intramolecular hairpin molecule remain constant despite the 60- to 160-fold increase in strand concentration, 5 μM to 800 μM (UV and DSC melts). This confirms the formation of unimolecular complexes at low temperatures. Furthermore, the much higher $t_m$'s of 71−79°C in 1 M NaCl (34) relative to the estimated $t_m$ of the d(GCGC)$_2$ duplex of 46°C in this salt concentration at 10 μM strand concentration, together with the similarity of the transition enthalpies and the observed increase in the counterion release of these molecules, provide strong evidence of the exclusive formation of intramolecular hairpins.

### Thermodynamic contribution of the thymine loops

An increase in the number of thymine residues in the loops results in a decreased stability of these molecules that is accompanied by similar enthalpic contributions of −38.5 kcal mol$^{-1}$. Therefore, the lower stability of the hairpins with 5 and 7 thymines in the loops is entropically driven and corresponds to decreased stacking interactions of the constrained thymines in the loops and/or between the loop-thymines and the C·G base-pairs at the loop end of the stem (9, 11, 18). We estimate an average loop contribution to the enthalpy of −4.4 (± 0.6) kcal mol$^{-1}$ per 5′-C-T$_n$-G-3′ loop by assuming a salt independent enthalpy of −34.1 for the helical stem of all three molecules (35). This is in good agreement with the value of −3.2 kcal mol$^{-1}$ reported earlier for dumbbell molecules containing 4 thymines in the loop (37). In this range of loop length, the overall thermodynamic contribution of each loop residue to the formation of these hairpins corresponds to: $\Delta\Delta G° = +0.53$ kcal mol$^{-1}$, $\Delta\Delta H = -0.03$ kcal mol$^{-1}$, and $\Delta(T\Delta S) = -0.55$ kcal mol$^{-1}$ per thymine residue.

### Intercalation of ethidium to the stem site

We obtained similar binding affinities of $\sim 10^6$ for the association of ethidium to the helical stem of these hairpin molecules: GCGC/GCGC. This ligand is intercalating in the center CG/CG base pair stack of this helical stem according to the 5′-Pyr-Pur-3′ sequence specificity determined previously (26), with an increase in the electrostatic contribution as the loop size increases as seen from their larger decreases in $K_b$ with increased salt concentration. This suggests that increasing the length of the loop from 3 to 7 thymine residues improves the overall stacking interactions of the ligand with the DNA base pairs, as seen by the increase in binding enthalpy of −1.2 kcal mol$^{-1}$ and −3.0 kcal mol$^{-1}$, for a step increase of 2 and 4 thymine residues, respectively. A better explanation for this effect is that the local unwinding of the helical stem upon ethidium binding induces an increase in stacking interactions of the loop thymines. Therefore, the presence of the loops has a small influence on the local helical structure of the stem of these hairpins, in agreement with previous thermodynamic investigations of the binding of netropsin to the helical stem of dumbbells (38).

### The inclusion of loops creates additional ethidium binding sites

As an experimental control, we have studied the interaction of ethidium to a $dT_5$ oligomer by UV and calorimetric titrations and found no binding at all (34). Therefore, the structure of the thymines located in the loops of DNA hairpins may provide additional weaker binding sites for ethidium as detected by the calorimetric titration curves and spectroscopic Job plots. The values of the binding free energies are very similar and correspond to the non-specific binding of this ligand. However, an increase in the length of the loops results in a favorable increase in the binding enthalpies that are nearly compensated with unfavorable entropic terms. Our thermodynamic studies cannot predict the structure of these weaker sites. We can speculate that the thymines in the loop of $T_3$ hairpin are outside or completely crowded inside the loop (the former may explain the lower stoichiometry obtained from Job plots); increasing the number of residues to 5 and 7 would result in a rearrangement of these thymines inside the loop with the formation of additional stacking

interactions, which are favorable for ethidium binding. These additional sites may be composed of the C·G base pairs at the end of the helical stem plus the adjacent two thymines of the loops forming a local duplex structure of a CT/TG base-pair stack and the constrained thymines of the loops.

## CONCLUSIONS

The helix−coil transition of single-stranded hairpins of varied loop length was characterized thermodynamically. The transition temperature of the oligomer used in these studies was independent of strand concentration and slightly dependent on salt concentration. This provides strong evidence for the monomolecular transition of a hairpin molecule to single strand. Furthermore, the high transition temperature (70°C), and a low enthalpy (40 kcal $mol^{-1}$) of this hairpin-coil transition are consistent with stable hairpin structures. At temperatures up to 40°C, the hairpin structure is the predominant species in solution.

Due to the increased thermal stability of the free hairpin molecule, we were able to study the interactions of ethidium with these hairpins. These molecules were able to accommodate up to three ligand molecules, one in the stem and two in the loop. Each hairpin contains two types of binding sites with different thermodynamic binding profiles, and for both types the thermodynamic driving force is enthalpic. The stem contains the stronger site and is characterized by thermodynamic profiles typical of intercalation sites. The loops of these molecules contain weaker binding sites for ethidium.

## ACKNOWLEDGMENTS

We thank Professor Louise Pape for critical reading of the manuscript. This work was supported by Grant GM42223 from the National Institute of Health.

## REFERENCES

1. Chastain,M. and Tinoco,I.,Jr (1991) *Prog. Nucleic Acid Res. Mol. Biol.* **41**, 131−177.
2. Draper,D.E. (1992) *Acc. Che. Res.* **25**, 201−207.
3. Maniatis,T., Ptashne,M., Beckman,K., Kleid,D., Flashman,S., Jeffrey,A. and Maurer,R. (1975) *Cell* **5**, 109−113.
4. Rosenberg,M. and Court,D. (1979) *Annu. Rev. Genet.* **13**, 319−351.
5. Wells,R.D., Goodman,T.C., Hillen,W., Hom,G.T., Klein,R.D., Larson,J.E., Muller,U.R., Neuendorf,S.K., Panayotatos,N. and Stirdivant,S.M. (1980) *Prog. Nucleic Acid Res. Mol. Biol.* **25**, 167−267.
6. Marky,L.A., Blumenfeld,K.S., Kozlowski,S. and Breslauer,K.J. (1983) *Biopolymers* **22**, 1247−1257.
7. Wemmer,D.E., Chou,S.H., Hare,D.R. and Reid,B.R. (1985) *Nucleic Acids Res.* **13**, 3755−3772.
8. Haasnoot,C.A.G., Hilbers,C.W., van der Marel,G.A., van Boom,J.H., Singh,U.C., Pattabiraman,N. and Kollman,P.A. (1986) *J. Biomol. Struct. Dyn.* **3**, 843−857.
9. Hare,D.R. and Reid,B.R. (1986) *Biochemistry* **25**, 5341−5350.
10. Ikuta,S., Chattopadhyaya,R., Dickerson,R.E. and Kearns,D.R. (1986) *Biochemistry* **25**, 4840−4849.
11. Gupta,G., Sarma,M.H., Sarma,R.H., Bald,R., Engelke,U., Oei,S.L., Gessner,R. and Erdmann,V.A. (1987) *Biochemistry* **27**, 7715−7723.
12. Wolk,S., Hardin,C.C., Germann,M.W. van de Sande,J.H. and Tinoco,I.,Jr (1988) *Biochemistry* **27**, 6960−6967.
13. Williamson,J.R. and Boxer,S.G. (1989) *Biochemistry* **28**, 2819−2831.
14. Williamson,J.R. and Boxer,S.G. (1989) *Biochemistry* **28**, 2831−2836.
15. Garcia,A.E., Gupta,G., Soumpasis,D.M. and Tung,C.S. (1990) *J. Biomol. Struct. Dyn.* **8**, 173−186.
16. Paner,T.M., Amaratunga,M., Doktycz,M.J. and Benight,A.S. (1990) *Biopolymers* **29**, 1715−1731.
17. Rentzeperis,D., Kharakoz,D.P. and Marky,L.A. (1991) *Biochemistry* **30**, 6276−6283.
18. Hilbers,C.W., Hasnoot,C.A.G., de Bruin,S.H., Joorden,J.J., van der Marel,G.A. and van Boom,J.H. (1985) *Biochimie* **67**, 685−695.
19. Senior,M.M., Jones,R.A. and Breslauer,K.J. (1988) *Proc. Nat. Acad. Sci. USA* **85**, 6242−6246.
20. Xodo,L.E., Manzini,G., Quadrifoglio,F., van der Marel,G.A. and van Boom,J.H. (1988) *Biochemistry* **27**, 6321−6326.
21. Amaratunga,M., Snowden-Ifft,E., Wemmer,D.E. and Benight,A.S. (1992) *Biopolymers* **32**, 865−879.
22. Antao,V.P. and Tinoco,I.,Jr (1992) *Nucleic Acid Res.* **20**, 819−824.
23. Krugh,T.R. and Reinhardt,G.C. (1975) *J. Mol. Biol.* **97**, 133−162.
24. Jovin,T.M. and Striker,G. (1977) *Mol. Biol. Biochem. Biophy.* **24**, 245−281.
25. Breslof,J.L. and Crothers,D.M. (1981) *Biochemistry* **20**, 3547−3533.
26. Krugh,T.R., Hook,J.W,III, Lin,S. and Chen,F. (1979) In Sarma,R.H. (ed.), *Stereodymanics of Molecular Systems*. Pergamon Press, NY, pp. 423−435.
27. Caruthers,M.H. (1982) In Gassen,H.G. and Lang,A. (eds.), *Chemical and Enzymatic Synthesis of Gene Fragments*. Verlag Chemie: Weinheim, Germany, pp. 71−79.
28. Cantor,C.R., Warshow,M.M. and Shapiro,H. (1970) *Biopolymers* **9**, 1059−1077.
29. Rentzeperis,D., Karsten,R., Jovin,T.M. and Marky,L.A. (1992) *J. Am. Chem. Soc.* **114**, 5926−5928.
30. Breslof,J.L. and Crothers,D.M. (1975) *J. Mol. Biol.* **95**, 103−123.
31. Marky,L.A. and Breslauer,K.J. (1987) *Biopolymers* **26**, 1601−1620.
32. Wiseman,T., Williston,S., Brandts,J.F. and Lin,L.N. (1989) *Anal. Biochem.* **179**, 131−137.
33. Crothers,D.M. (1971) *Biopolymers* **10**, 2147−2160.
34. Rentzeperis,D. and Marky,L.A. (unpublished).
35. Breslauer,K.J., Frank,R., Blöcker,H. and Marky,L.A. (1986) *Proc. Nat. Acad. Sci. USA* **83**, 3746−3750.
36. Zieba,K., Chu,T.M., Kupke,D.W. and Marky,L.A. (1991) *Biochemistry* **30**, 8018−8026.
37. Record,M.T.,Jr, Anderson,C.F. and Lohman,T.M. (1978) *Q. Rev. Biophys.* **11**, 103−178.
38. Rentzeperis,D., Ho,J. and Marky,L.A. (1993) *Biochemistry* **32**, 2564−2572.
39. Paner,T.M., Amaratunga,M. and Benight,A.S. (1992) *Biopolymers* **32**, 881−892.
40. Waring,M.J. (1965) *J. Mol. Biol.* **13**, 269−282.
41. Boulard,Y., Gabarro-Arpa,J., Cognet,J.A.H., Le Bret,M., Guy,A., Téoule,R., GuschlbauerR. and Fazakerley,G.B. (1991) *Nucleic Acids Res.* **19**, 5159−5167.
42. Chou,W.Y., Marky,L.A., Zaunczkowski,D. and Breslauer,K.J. (1987) *J. Biomol. Struct. Dyn.* **5**, 345−359.
43. Friedman,R.A. and Manning,G.S. (1984) *Biopolymers* **23**, 2671−2714.